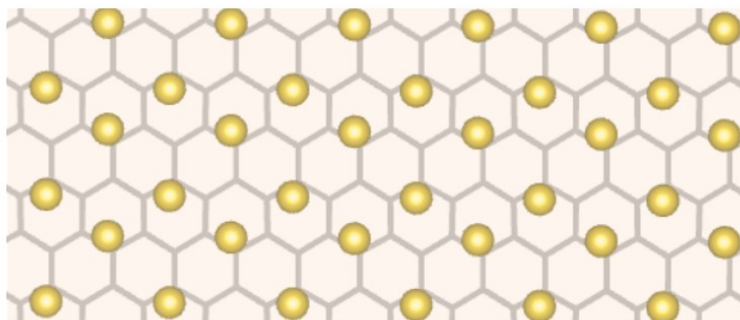
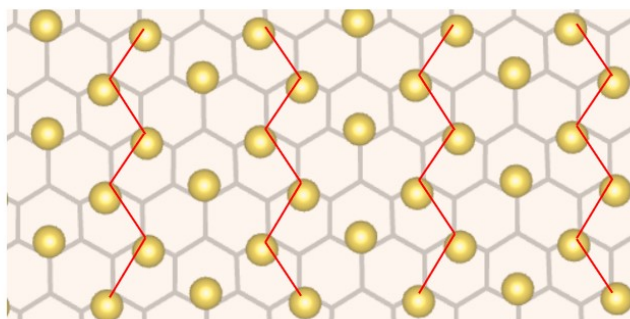


## Supplementary Materials

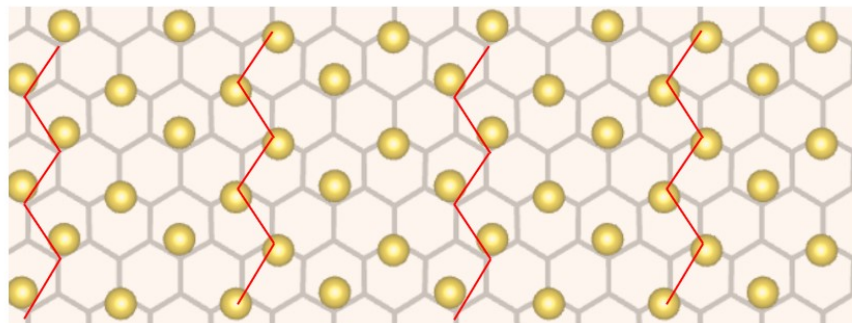
$$x_{NDW} = 1/2$$



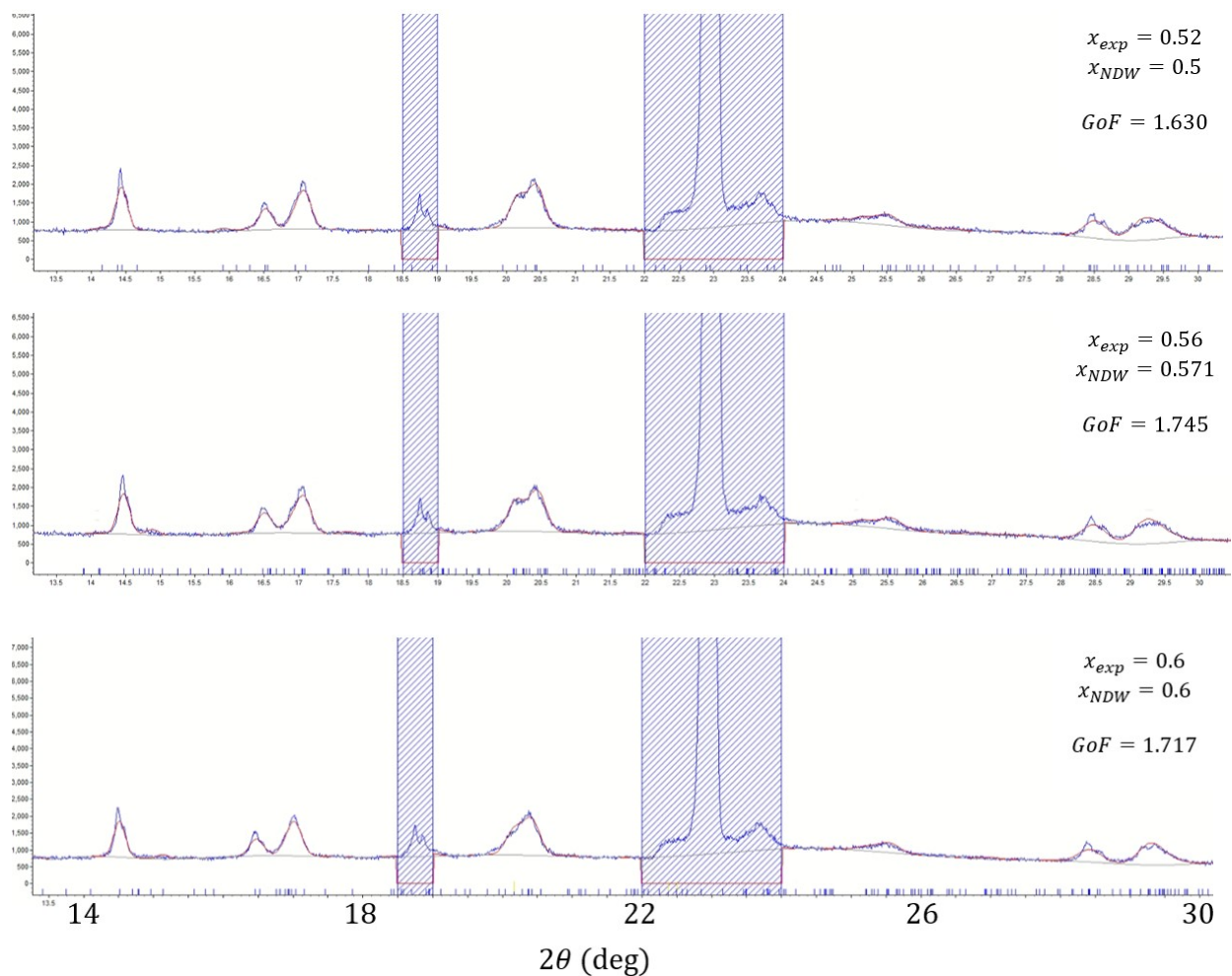
$$x_{NDW} = 3/5$$



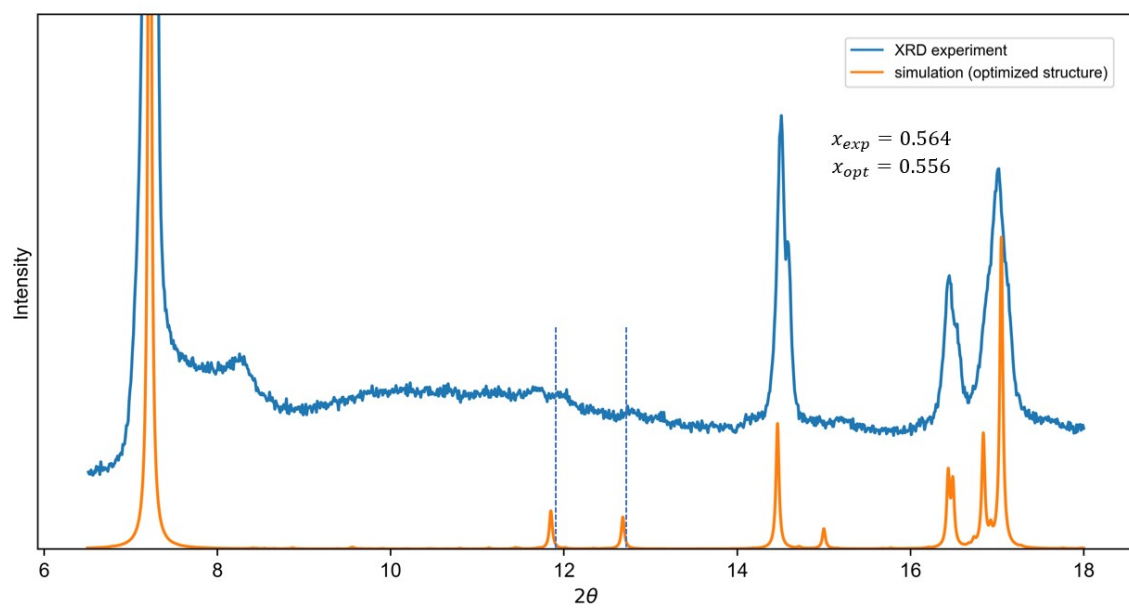
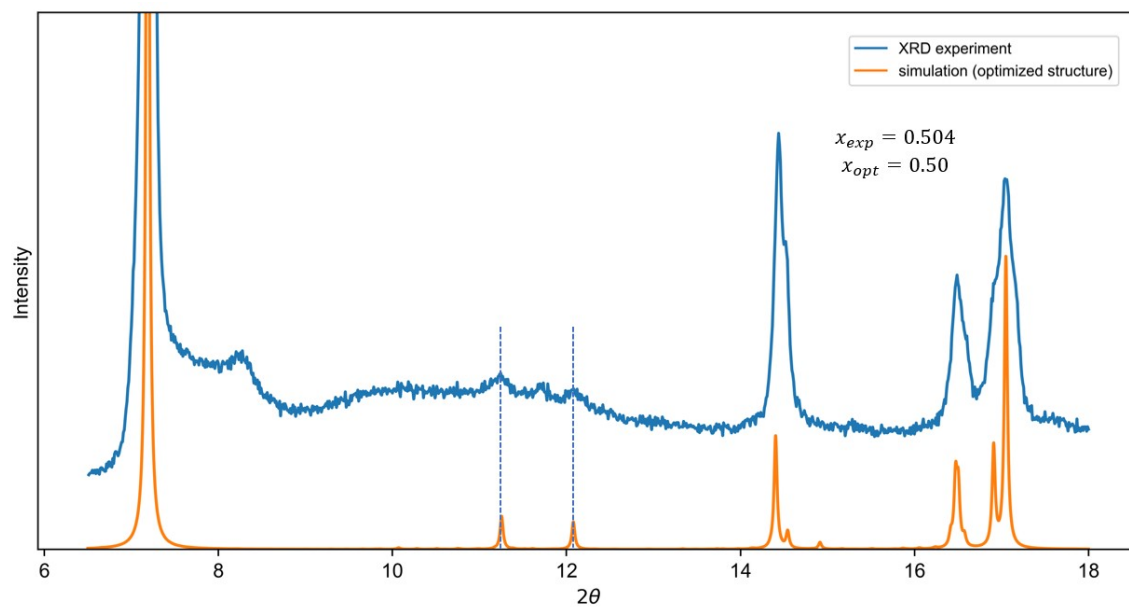
$$x_{NDW} = 4/7$$

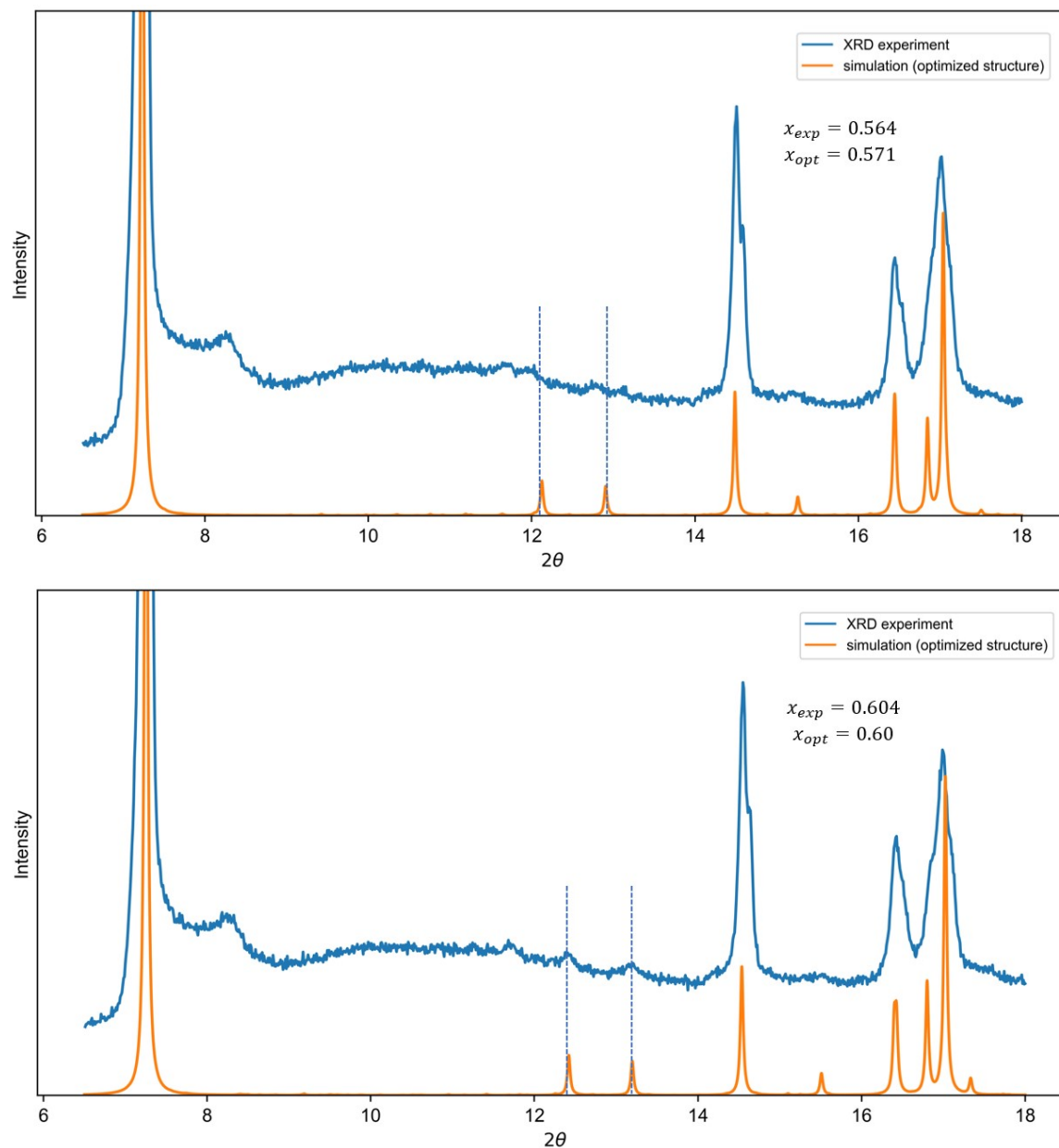


**Fig S1.** Structure of Na density wave (NDW) pattern at  $x > 0.5$  in battery charge as reported in literature[1]. Red lines connect sites with shorter distance that form the high-density regions in the NDW.

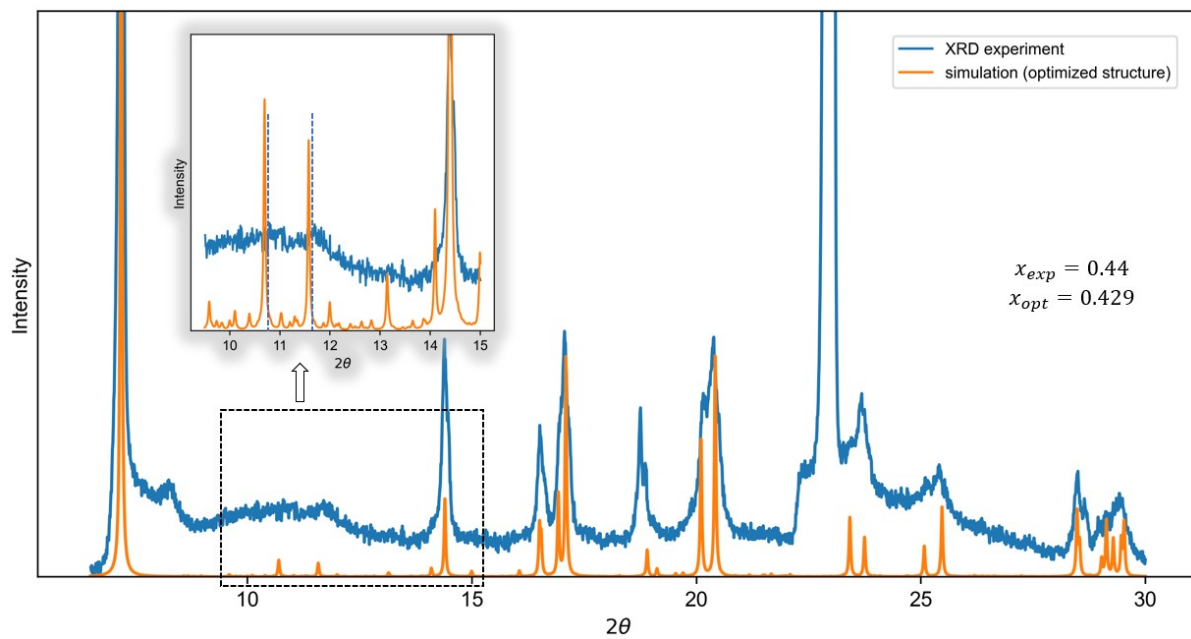
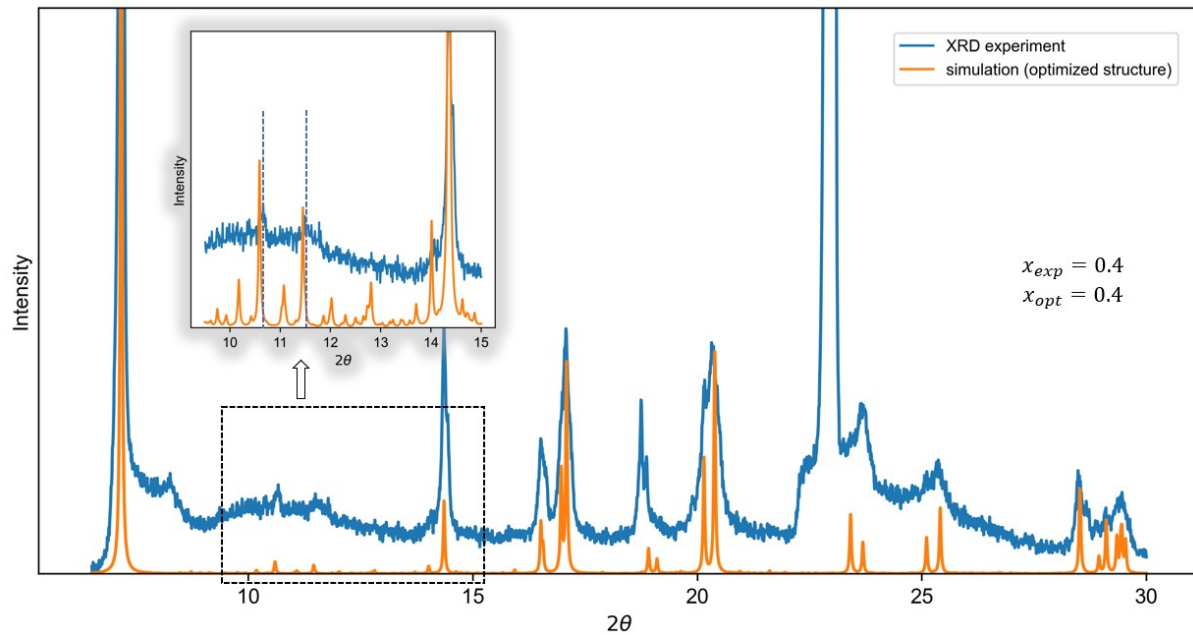


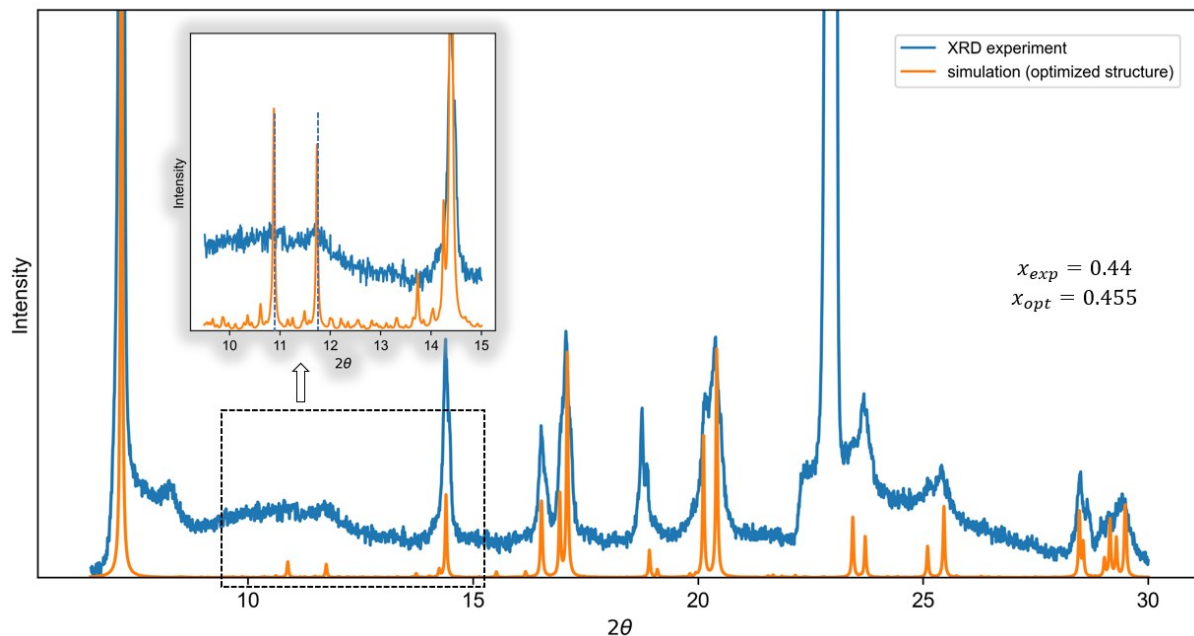
**Fig S2.** *In situ* XRD (Mo source) refinement results for Na Density Wave (NDW) structures of  $x_{NDW} = 1/2$ ,  $4/7$ , and  $3/5$  using the *in situ* XRD in the second charge. Shadow background part is excluded from the refinement. The peaks at  $\sim 18.7^\circ$  and between  $22^\circ \sim 24^\circ$  are from *in situ* cell components (e.g., electrolyte, Al current collect, glass fiber, steel cell case, and Be window).



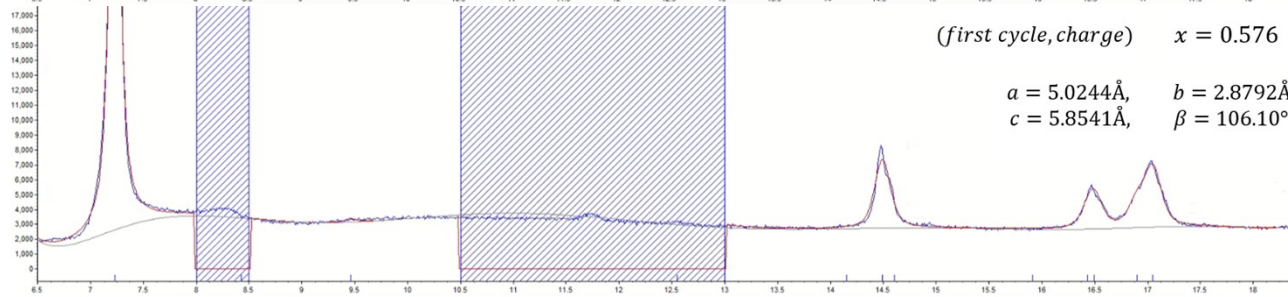
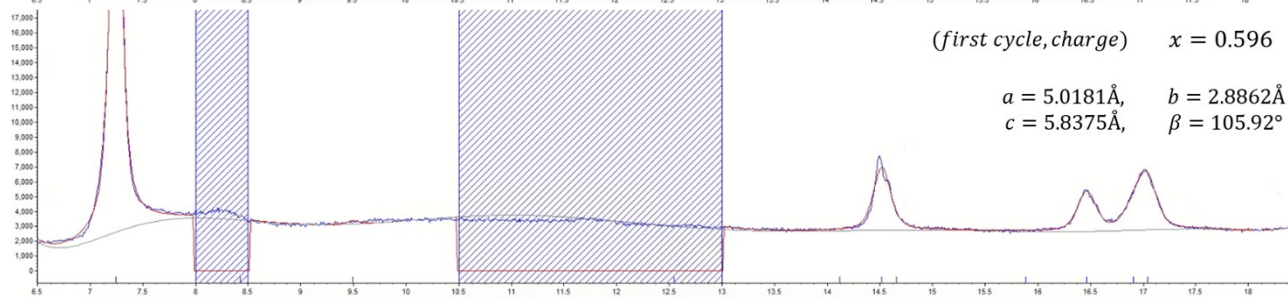
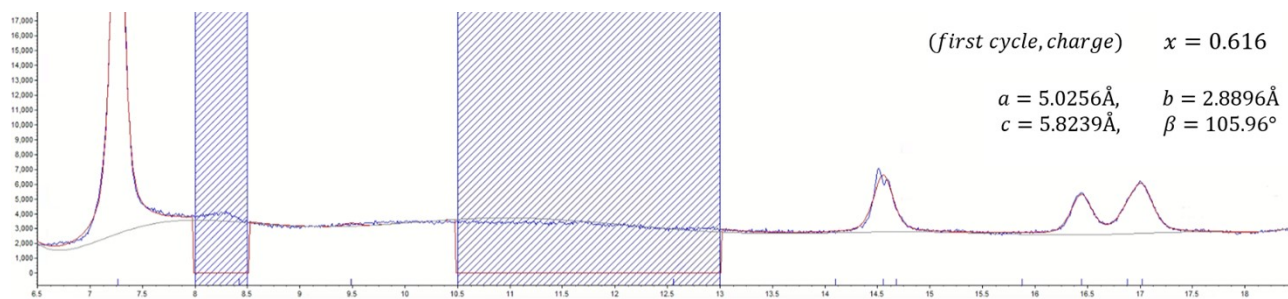
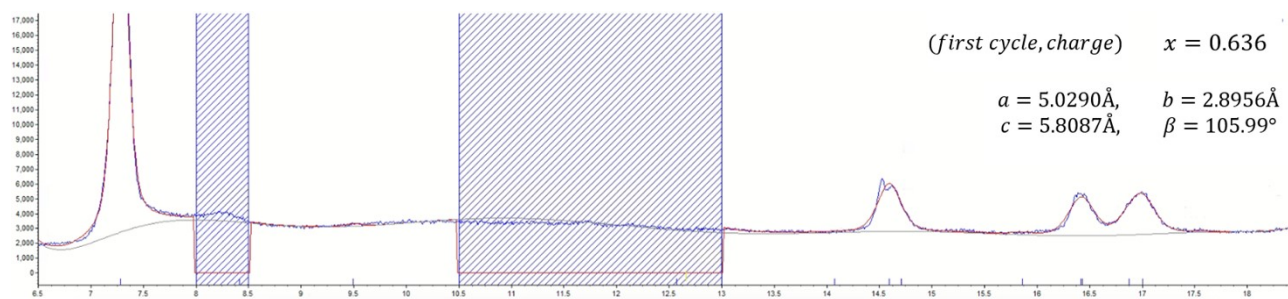


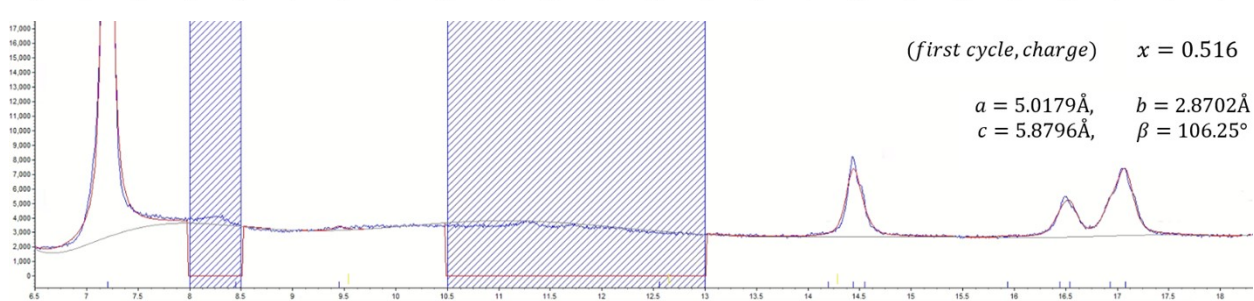
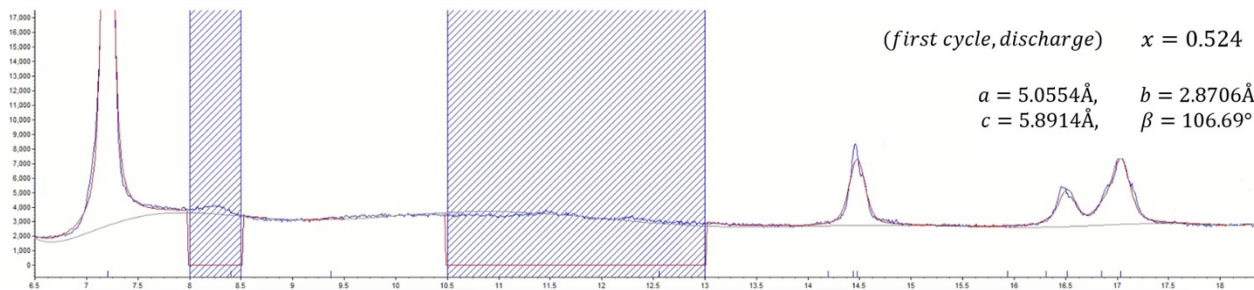
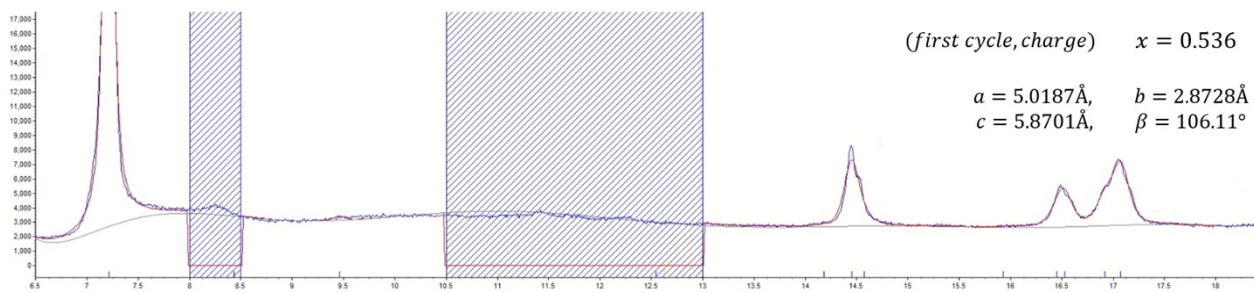
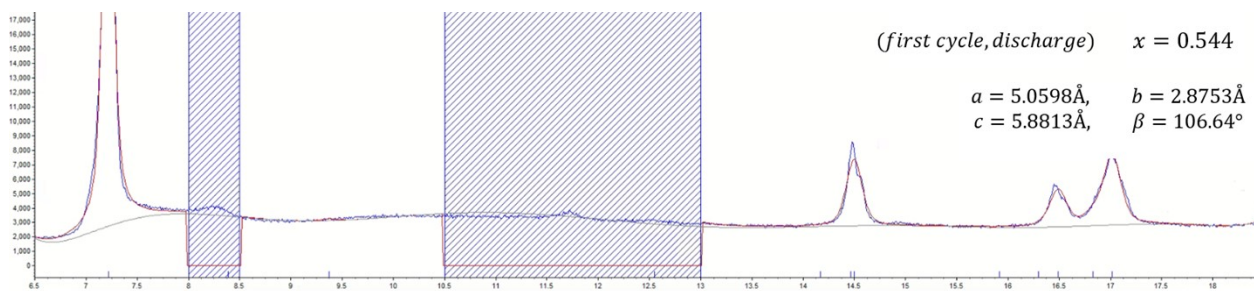
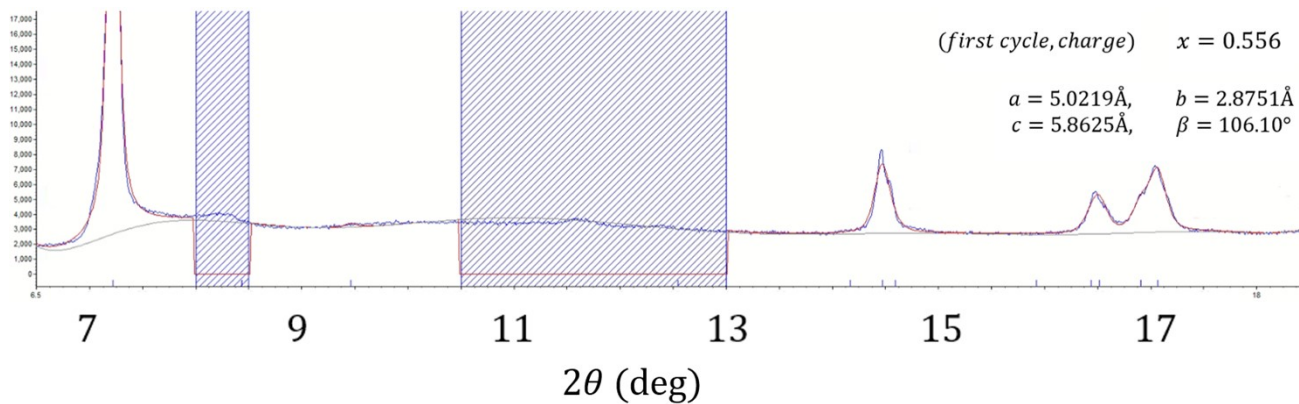
**Fig S3.** Experimental *in situ* XRD pattern (Mo source) in comparison with simulated XRD pattern from supercells of optimized Na positions. Simulation of optimized structures in the first cycle (discharge).  $x_{exp}$  and  $x_{opt}$  refer to compositions in experiment and in optimized structure, respectively. Blue vertical dashed line is the expected peak position from experiment. For those compositions that cannot match, i.e.,  $x_{exp} \neq x_{opt}$ , the expected peak position is obtained from linear interpolation of experimental lattice parameters from two neighboring *in situ* XRD patterns, as described in the text.

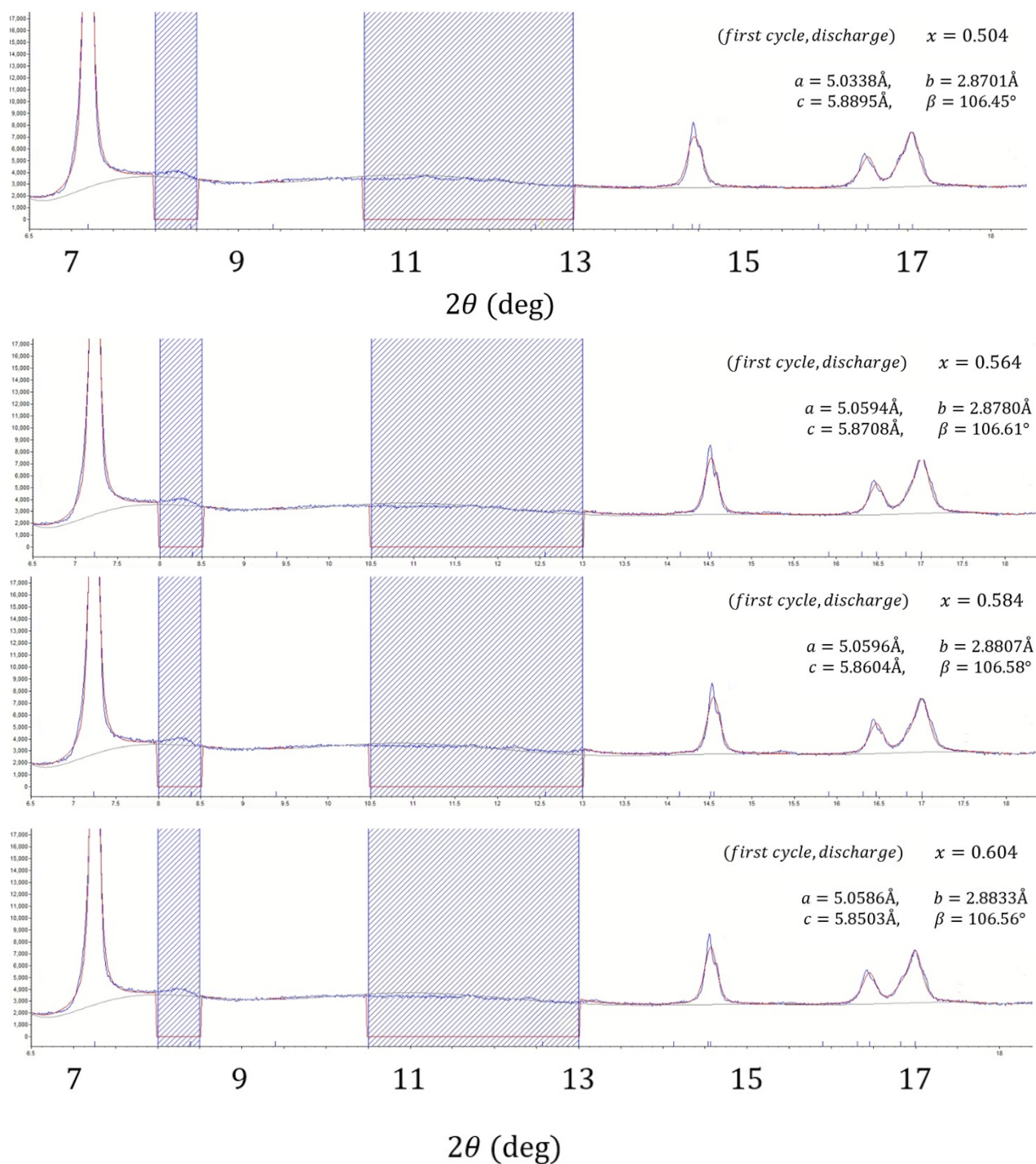




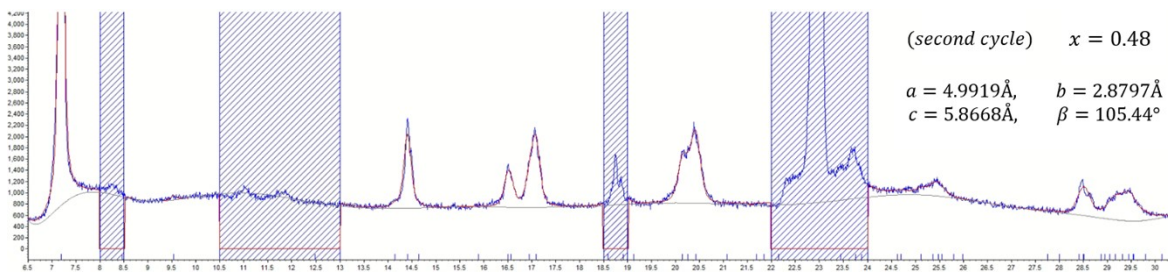
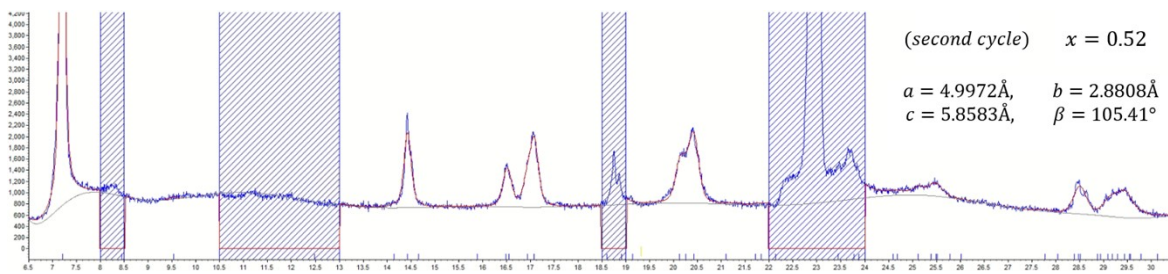
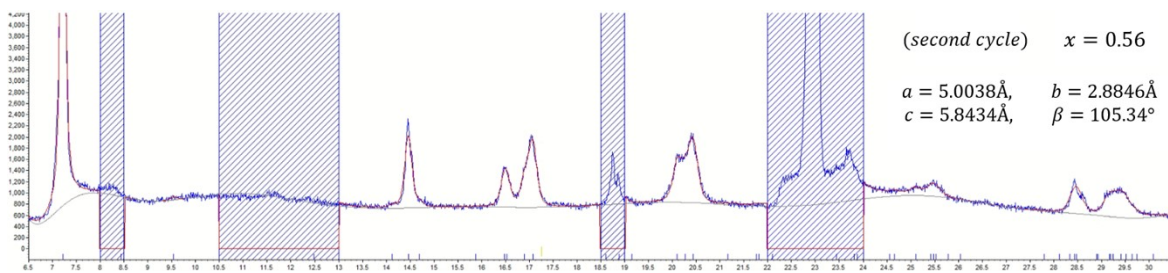
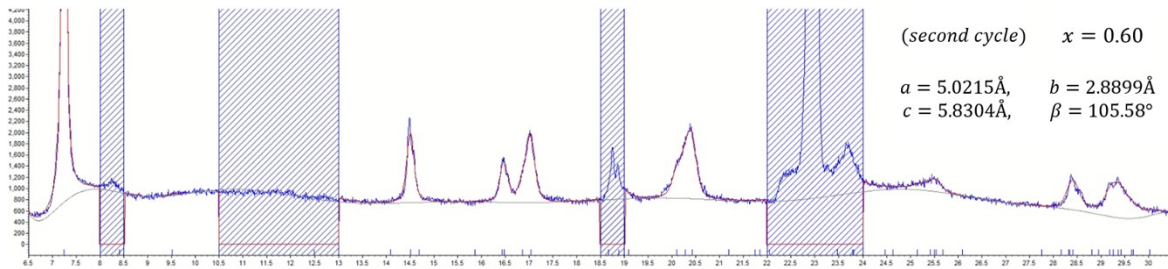
**Fig S4.** Experimental *in situ* XRD pattern (Mo source) in comparison with simulated XRD pattern from supercells of optimized Na positions. Simulation of optimized structures in the second charge.  $x_{exp}$  and  $x_{opt}$  refer to sodium compositions in experiment and in optimized structure, respectively. Blue vertical dashed line is the expected peak position from experiment. For those compositions that cannot match, i.e.,  $x_{exp} \neq x_{opt}$ , the expected peak position is obtained from linear interpolation of experimental lattice parameters from two neighboring *in situ* XRD patterns, as described in the text.







**Fig S5.** Pawley refinement fits to obtain lattice parameters from *in situ* XRD (Mo source) patterns in the first cycle. Blue curves are experimental data and red curves are simulations. Shadow background part is excluded from the refinement. The peak at  $\sim 8.2^\circ$  is from *in situ* cell components (e.g., PTFE binder). The region of superstructure peaks between  $10.5^\circ\sim 13^\circ$  is also not considered here.



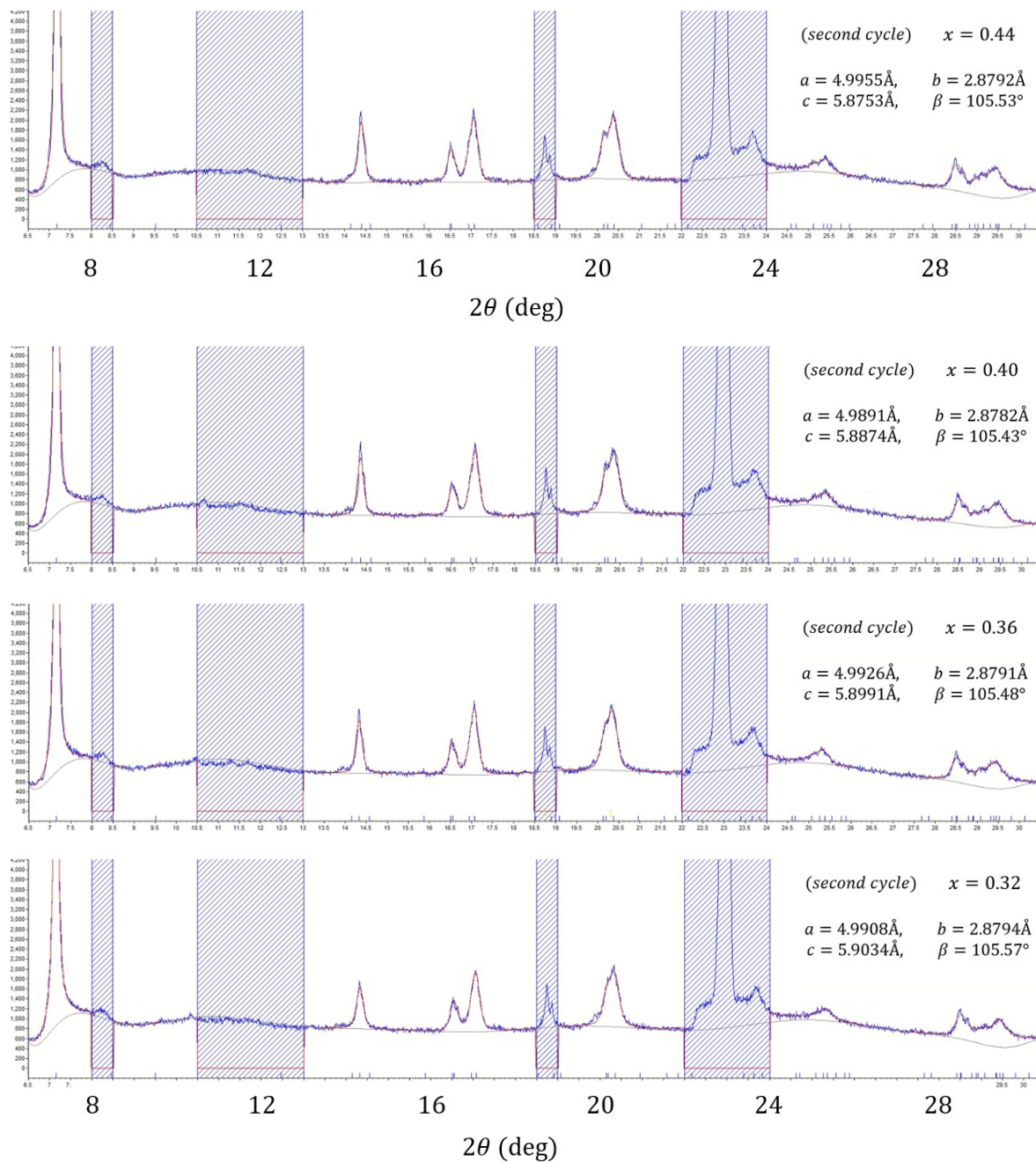


**Fig S6.** Results of *in situ* XRD (Mo source) refinement of lattice parameters for the second charge. Blue curves are experimental data and red curves are simulations. Shadow background part is excluded. The peaks at  $\sim 8.2^\circ$ , at  $\sim 18.7^\circ$ , and between  $22^\circ\sim 24^\circ$  are from *in situ* cell components (e.g., PTFE binder, electrolyte, Al current collect, glass fiber, steel cell case, and Be window). The region of superstructure peaks between  $10.5^\circ\sim 13^\circ$  is also not considered here.

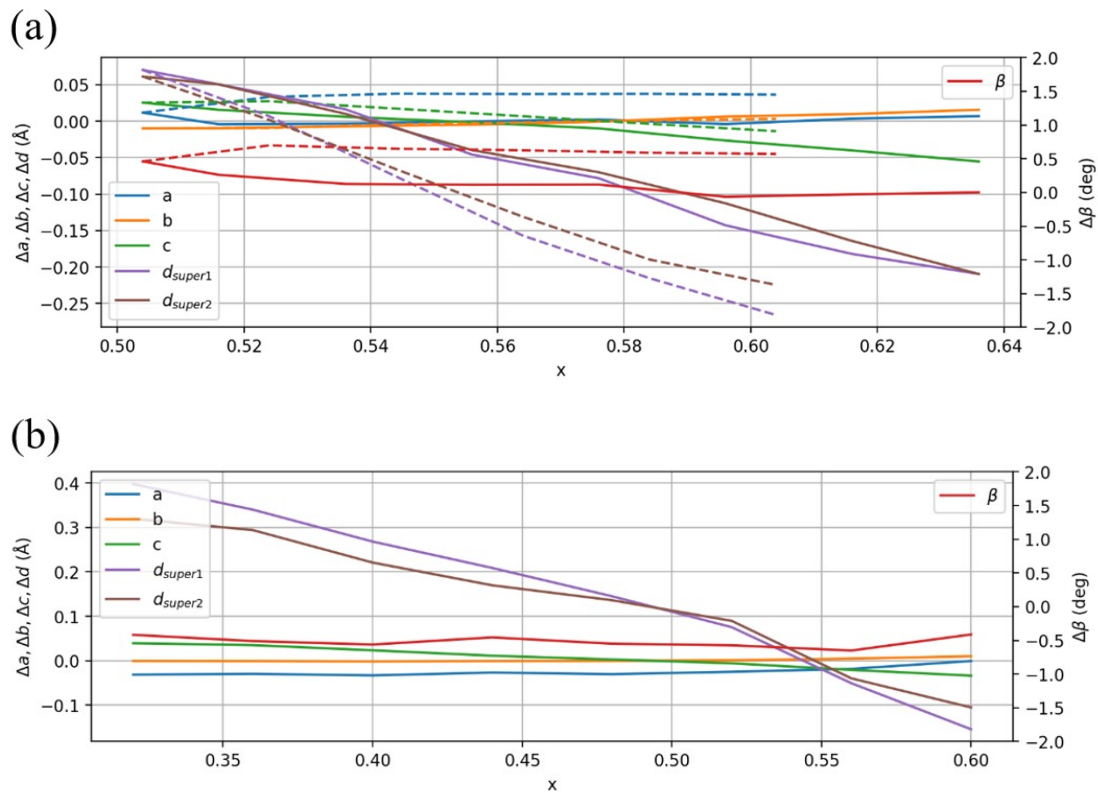


**Fig S7.** Lattice parameters from *in situ* XRD refinement at different Na composition  $x$ . The plots show variations from mean values

$$a = 5.0221\text{\AA}, b = 2.8799\text{\AA}, c = 5.8640\text{\AA}, \beta = 105.99^\circ, d_{super1} = 3.5499\text{\AA}, d_{super2} = 3.3117\text{\AA},$$

where  $d_{super1}$  and  $d_{super2}$  are the corresponding  $hkl$  plane distances of the two characteristic superstructure peaks from *in situ* XRD. We see that compare with the shift of superstructure peaks, the change of lattice parameters are very small. (a) Result of the first cycle. Charge process is in solid line and discharge process is in dashed line. (b) Result of the second charge.

Direction	Coupling coefficients	Value ( $meV/\mu_s^2$ )
horizontal	$J_{12}$	-2.4
	$J_{23}$	-2.7
	$J_{34}$	-1.2
diagonal	$J_{25} + J_{36}$	-3.1
	$J_{26}$	-0.6
	$J_{37} + J_{38}$	-1.4

**Table S1.** DFT calculated magnetic coupling coefficients in the structure of Fig 6.

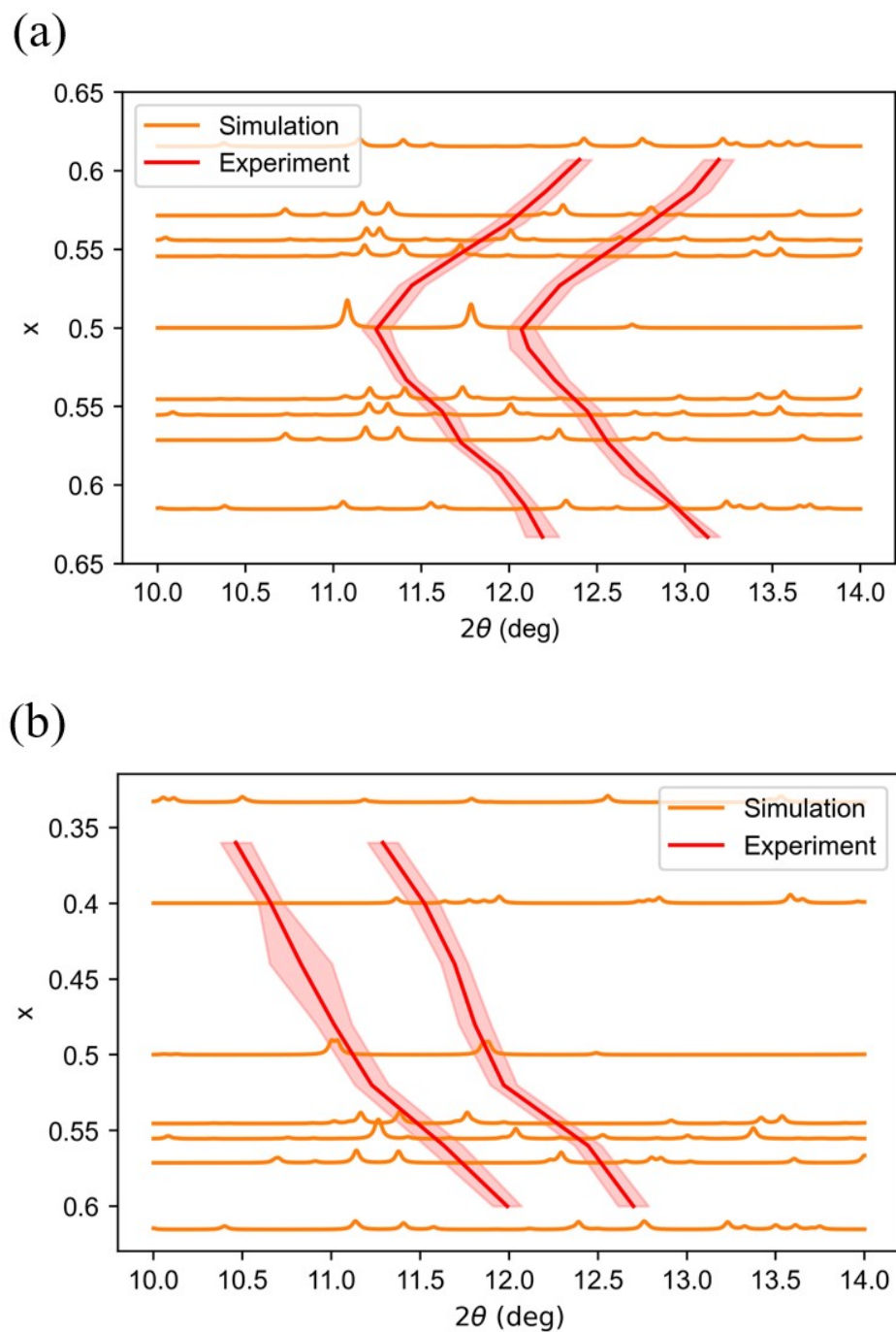


**Fig S8.** Comparison of superstructure peaks between simulated XRD spectra from DFT ground state structures in literature [2] and our *in situ* XRD experiment result. **(a)** Result of the first cycle. **(b)** Result of the second charge. Red lines indicate positions of superstructure peaks in experiment and the error bar of the red region is from FWHM of the superstructure peak. Lattice parameters of the DFT supercells have been first imposed with the values obtained from *in situ* XRD refinement to match main XRD *hkl* peaks, and then perform the simulation of superstructure peaks in orange here.

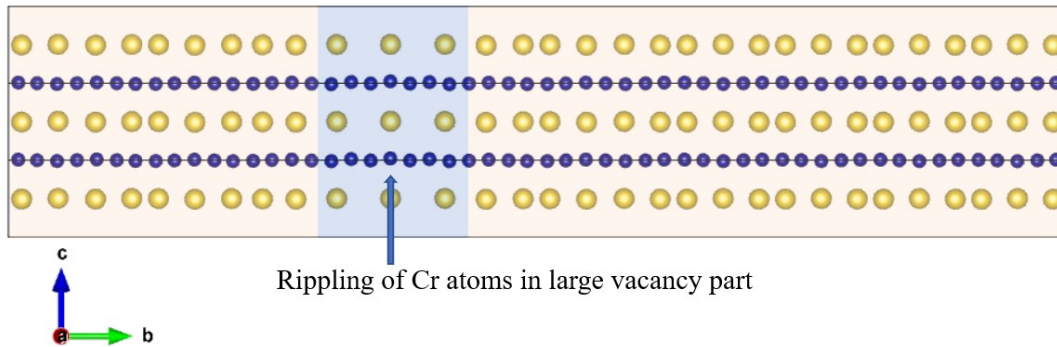


**Fig S9.** Small Cr atom rippling from DFT relaxed structure at  $x_{opt} = 5/9$ . The variation in the  $z$  direction for the Cr atom marked by the arrow is only  $0.14 \text{ \AA}$ .

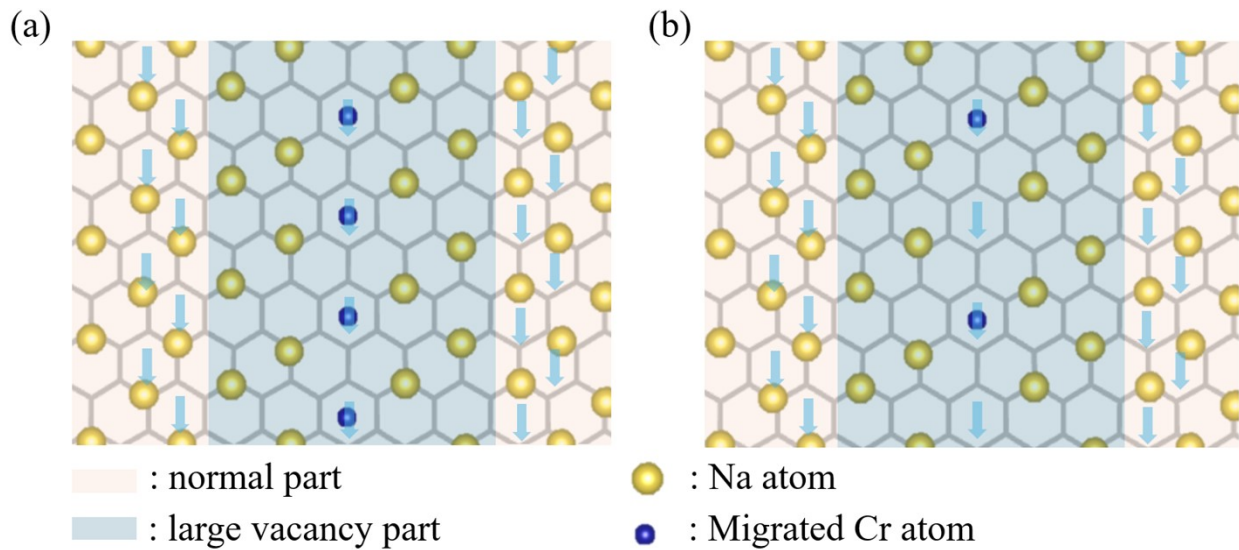


**Fig S10.** Schematic illustration of Cr migration coupled with nano-strips of large vacancy structures. (a) Complete (100%) Cr migration in a line along the  $a$  direction. (b) Alternating (50%) Cr migration in a line along the  $a$  direction. Blue spheres represent Cr atoms migrated from the transition metal oxide layer to the Na ion layer. Downward arrows indicate down-spins associated with local magnetic ordering, and Cr sites without arrows correspond to up-spins.

## Reference

[1] X. Chen, H. Tang, Y. Wang, and X. Li, Balancing orbital effects and on-site Coulomb repulsion through

Na modulations in  $\text{Na}_x\text{VO}_2$ , *Phys. Rev. Mater.* 2021, 5, 084402

[2] Kaufman JL, Van der Ven A. First-principles investigation of phase stability in layered  $\text{Na}_x\text{CrO}_2$ . *Physical Review Materials*. 2022 Nov 1;6(11):115401.